Effects of Magnesium on Inactivation of the Voltage-gated Calcium Current in Cardiac Myocytes

H. CRISS HARTZELL and RICHARD E. WHITE

From the Department of Anatomy and Cell Biology, Emory University School of Medicine, Atlanta, Georgia 30322

ABSTRACT The effects of changes in intracellular and extracellular free ionized [Mg^{2+}] on inactivation of I_{Ca} and I_{Ba} in isolated ventricular myocytes of the frog were investigated using the whole-cell configuration of the patch-clamp technique. Intracellular [Mg^{2+}] was varied by internal perfusion with solutions having different calculated free [Mg^{2+}]. Increasing $[Mg^{2+}]_i$ from 0.3 mM to 3.0 mM caused a 16% reduction in peak I_{Ca} amplitude and a 36% reduction in peak I_{Ba} amplitude, shifted the current-voltage relationship and the inactivation curve ~10 mV to the left, decreased relief from inactivation, and caused a dramatic increase in the rate of inactivation of I_{Ba}. The shifts in the current-voltage and inactivation curves were attributed to screening of internal surface charge by Mg^{2+}. The increased rate of inactivation of I_{Ba} was due to an increase in both the steady-state level of inactivation as well as an increase in the rate of inactivation, as measured by two-pulse inactivation protocols. Increasing external [Mg^{2+}] decreased I_{Ba} amplitude and shifted the current-voltage and inactivation curves to the right, but, in contrast to the effect of internal Mg^{2+}, had little effect on the inactivation kinetics or the steady-state inactivation of I_{Ba} at potentials positive to 0 mV. These observations suggest that the Ca channel can be blocked quite rapidly by external Mg^{2+}, whereas the block by $[Mg^{2+}]_i$ is time and voltage dependent. We propose that inactivation of Ca channels can occur by both calcium-dependent and purely voltage-dependent mechanisms, and that a component of voltage-dependent inactivation can be modulated by changes in cytoplasmic Mg^{2+}.

INTRODUCTION

Magnesium is an important constituent of the intracellular milieu. Despite the importance of magnesium as an essential cofactor in hundreds of enzymatic reactions and other cellular processes, relatively little is known about the regulation of intracellular [Mg^{2+}] or the regulation of cellular processes by physiological changes in the concentration of free ionized magnesium ($[Mg^{2+}]_i$). It seems unlikely that

Address reprint requests to Dr. H. Criss Hartzell, Department of Anatomy and Cell Biology, Emory University School of Medicine, Atlanta, GA 30322.

Dr. White's present address is Laboratory of Cellular and Molecular Pharmacology, NIEHS, Research Triangle Park, NC 27709.

J. GEN. PHYSIOL. © The Rockefeller University Press · 0022-1295/89/10/0745/23 $2.00
Volume 94 October 1989 745–767

magnesium acts as a "trigger" of enzymatic processes as does calcium, however, a variety of evidence now suggests that magnesium does play a role in long-term cellular regulation (see reviews by Flatman, 1984; Gupta et al., 1984; White and Hartzell, 1989). $[Mg^{2+}]_i$ is far from thermodynamic equilibrium in most cells (Flatman, 1984; Gupta et al., 1984; Alvarez-Leefmans et al., 1986), and can be altered under a variety of physiological conditions (Gupta et al., 1978; Cech et al., 1980; Gupta and Yushok, 1980; Alvarez-Leefmans et al., 1986). Furthermore, specific magnesium transport systems have been identified in several cell types, and in a few cases these transport systems are hormonally regulated (Henquin et al., 1983; Maguire, 1984). These findings support the suggestion that $[Mg^{2+}]_i$ and, therefore, Mg-dependent reactions may be actively regulated. Despite the evidence that cellular $[Mg^{2+}]$ may vary, there is very little data on the physiological effects of changing $[Mg^{2+}]_i$ within a physiological range.

We (White and Hartzell, 1988) have recently reported that changing intracellular free ionized magnesium in isolated cardiac cells by internal perfusion has dramatic effects on the voltage-gated calcium current, I_{Ca}. In these experiments we showed that changing $[Mg^{2+}]_i$ within a physiological range of 0.3 to 3.0 mM decreased the amplitude of basal I_{Ca} by 20%, but decreased the amplitude of I_{Ca} elevated by cAMP-dependent phosphorylation even more, by 63%. This effect of $[Mg^{2+}]_i$ on cAMP-elevated I_{Ca} was shown to be due largely to processes beyond Ca channel phosphorylation, because Ca currents elevated by various procedures including β-receptor stimulation, internal perfusion with cAMP, internal perfusion with nonhydrolyzable analogues of cAMP such as 8Br-cAMP, or internal perfusion with the purified catalytic subunit of cAMP-dependent protein kinase were all affected similarly by changes in $[Mg^{2+}]_i$. These results suggested that the effect of $[Mg^{2+}]_i$ could not be explained simply by changes in cAMP levels. We proposed the hypothesis that $[Mg^{2+}]_i$ stimulates a protein phosphatase that dephosphorylates the Ca channel, or that Mg^{2+} interacts directly with the Ca channel.

This paper explores in more detail the effects of $[Mg^{2+}]_i$ on Ca channels. In order to gain insights into the mechanism of Mg^{2+} action, we have examined the effects of internal and external $[Mg^{2+}]$ on the inactivation of inward currents through Ca channels with either Ca^{2+} or Ba^{2+} as charge carrier. Inactivation of I_{Ca} consists of two components: a voltage-dependent mechanism analogous to Na channel inactivation, and a Ca-dependent mechanism that is linked to Ca^{2+} influx through the channel (see Brown et al., 1981; Eckert and Chad, 1984; Kass et al., 1986). When Ba^{2+} is used as the charge carrier, inactivation is due primarily to the voltage-dependent process. From our studies, we conclude that increasing $[Mg^{2+}]_i$ causes a marked increase in the rate and extent of voltage-dependent inactivation of Ca channels. We propose that internal Mg^{2+} can block Ca channels in a time- and voltage-dependent fashion, and that this block could be partly responsible for "voltage-dependent" inactivation.

METHODS

Electrophysiology

I_{Ca} was measured in single isolated myocytes from frog ventricle using the whole-cell configuration of the patch-clamp technique (Hamill et al., 1981) by methods described in detail

(Fischmeister and Hartzell, 1987; Hartzell and Simmons, 1987; Argibay et al., 1988). I_{Na} was blocked with tetrodotoxin (TTX). K^+ currents were suppressed by both internal and external Cs^+. Sometimes internal tetraethyl ammonium (TEA) was also used. Currents were elicited by 200 or 400 ms duration voltage pulses. I_{Ca} was measured as the peak inward current minus the quasi–steady-state current at the end of the 200- or 400-ms pulse (steady-state current, I_{ss}). When Ba^{2+} was used as a charge carrier, I_{Ba} did not inactivate completely during the pulse. Under these conditions, I_{Ba} was calculated as the difference between the peak inward current and the current at the end of an identical pulse in Ca^{2+}, 2.0 mM Cd^{2+}, or 1.0 μM nifedipine. These three methods gave similar, though not identical results. I_{ss} with Ca^{2+} as charge carrier was sometimes 10–20 pA more outward than with the other two methods. This may reflect an outward nonspecific current that is blocked by Cd^{2+} (Brown et al., 1981) in some cells. To block this outward component of the current, 20 mM CsCl in the internal solution was replaced with 20 mM TEA-Cl in some experiments. The effects of magnesium were not significantly affected by the addition of TEA-Cl. In some experiments, the currents were leak subtracted. Leak was determined by averaging several current traces evoked by voltage pulses from -80 to -70 mV. The mean holding current and leak current were calculated from the averaged trace and used to construct an idealized noise-free leak trace. The trace was then multiplied by the appropriate scaling factor, assuming a linear current-voltage relationship for the leak, and subtracted from the I_{Ca} or I_{Ba} traces. The voltage protocols for determining I_{Ca} inactivation are based on the two-pulse paradigm of Hodgkin and Huxley (1952) and are published (Fischmeister and Hartzell, 1986; Argibay et al., 1988). The protocols are also described here in the figure legends. Half-inactivation was defined as the prepulse potential producing 50% of the inactivation produced by the same duration prepulse to 0 mV.

Solutions

Two different external solutions were used with identical results. HCO_3-buffered Ringers contained 88 mM NaCl, 20 mM CsCl, 0.6 mM Na_2PO_4, 24 mM $NaHCO_3$, 1.8 mM $MgCl_2$, 1.8 $CaCl_2$ or 2 mM $BaCl_2$, 5 mM sodium pyruvate, 5 mM glucose, 0.001 mM TTX, pH 7.4 with 95% O_2–5% CO_2. HEPES-buffered Ringers contained 115 NaCl, 20 mM CsCl, 0.3–3.0 mM $MgCl_2$, 1.8 mM $CaCl_2$ or 2 mM $BaCl_2$, 5 mM sodium pyruvate, 5 mM glucose, 0.001 mM TTX, 10 mM HEPES (*N*-2-hydoxyethyl-piperazine-*N'*-2-ethane sulfonic acid), pH 7.4. External $[Mg^{2+}]$ was varied between 0.3 mM and 3 mM without compensation for changes in osmotic strength. When Ba^{2+} was used as charge carrier, Ca^{2+} was absent. The internal solution varied in composition and could be changed during recording by a system permitting continuous perfusion of the patch electrode (Hartzell and Fischmeister, 1986; Fischmeister and Hartzell, 1987).

The goal of these experiments was to examine the effects of changing free intracellular $[Mg^{2+}]$ while maintaining other ion concentrations as constant as possible. Composition of the solutions was calculated by a computer program developed by Godt and Lindley (1982), which was kindly provided by Dr. Robert Godt (Medical College of Georgia, Augusta, GA). The stability constants were the same as those published by Godt and Lindley (1982). In these calculations, we assumed that Cs^+ was equivalent to K^+. Recently, the free ion compositions of the solutions made with the Godt and Lindley program were recalculated using programs developed and kindly provided by Dr. Alexandre Fabiato (Medical College of Virginia, Richmond, VA) (Fabiato, 1988) using his preferred absolute stability constants. There were some differences in the absolute concentrations provided by these two calculations, but both calculations indicate that the [MgATP] concentration is constant (within 5% error), and $[Mg^{2+}]$ varies approximately 10-fold from the lowest to the highest $[Mg^{2+}]$ solution. Table I shows the composition of these solutions.

Exponential Curve Fitting

Currents were fitted to sums of exponentials by a Marquart least-squares procedure (FIT program, W. Goolsby, Emory University, Atlanta, GA). Leak-subtracted currents were used for least-squares fitting routine, and the current between the peak inward current and the end of the pulse was subjected to the curve-fitting routine.

RESULTS

Effects of Mg on Basal I_{Ca} and I_{Ba}

The effects of changing $[Mg^{2+}]_i$ on basal I_{Ca} and I_{Ba} are illustrated in Fig. 1. Currents were evoked by 400-ms voltage pulses from −80 to 0 mV at 8-s intervals. Net I_{Ca} and I_{Ba} were measured as described in Methods, and are plotted as a function of

TABLE I

Composition of Internal Solutions

Nominal $[Mg^{2+}]$ concentration	0.3 mM	1.0 mM	3.0 mM
	Total component concentration		
CsCl	116.8	118.3	113.5
K.PIPES	10.0	10.0	10.0
K_2EGTA	5.0	5.0	5.0
Na_2K_2ATP	3.26	2.80	2.67
$MgCl_2$	3.04	4.04	6.82
Na_2 creatine phosphate	5.0	5.0	5.0
pH	7.15	7.15	7.15
	*Calculated ion concentrations**		
MgATP	2.60 (2.47)	2.60 (2.51)	2.60 (2.56)
$[Mg^{2+}]$	0.30 (0.43)	1.00 (1.17)	3.00 (3.31)
ATP^{4-}	0.250 (0.49)	0.075 (0.18)	0.025 (0.065)
H_2EGTA	4.84	4.67	4.24
Ionic strength	190.0	190.0	190.0

All values are in millimolar. K.PIPES and K_2EGTA were made from their respective acids and titrated to pH 7.0 with KOH. Na_2K_2ATP was made from the disodium salt and titrated to pH 7.0 with KOH.

*Ion concentrations were calculated with a computer program developed by Godt and Lindley (1982) using their stability constants. The numbers in parentheses are the values obtained from Dr. Fabiato's program (1988) using his stability constants.

time in Fig. 1 *A*. At four times (marked *IV*) current-voltage relationships were determined by a series of voltage pulses from −50 to +50 mV. The cell was first perfused internally with a solution containing 0.3 mM $[Mg^{2+}]_i$ and superfused with Ringer solution containing 1.8 mM $CaCl_2$. When Ca^{2+} was replaced with 2.0 mM Ba^{2+}, the amplitude of the current increased about threefold. Changing the internal perfusion to a solution containing 3.0 mM $[Mg^{2+}]_i$ produced a 38% decrease in I_{Ba}, whereas I_{Ca} decreased less. The effects of $[Mg^{2+}]_i$ on the amplitude of I_{Ba} were quite variable and seemed to depend in part upon the order in which the internal solutions were used. When $[Mg^{2+}]_i$ was changed from 0.3 to 3.0 mM, I_{Ca} amplitude usually changed relatively little, but I_{Ba} amplitude was variably decreased (the range was 9–68% decrease). On the average, I_{Ca} was 16% smaller and I_{Ba} was 36% smaller in 3.0 mM $[Mg^{2+}]_i$ than in 0.3 mM $[Mg^{2+}]_i$ (Table II). In contrast, when the solution

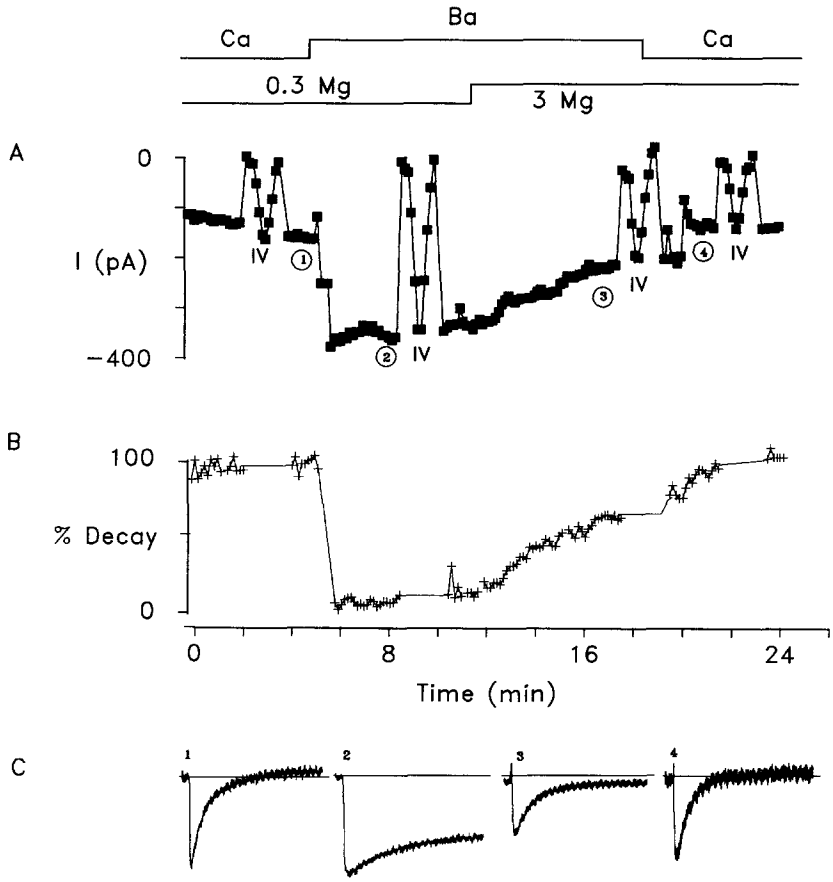

FIGURE 1. Effects of changing $[Mg^{2+}]_i$ on I_{Ca} and I_{Ba}. The cell was superfused with Ringer solution containing either 1.8 mM $CaCl_2$ or 2 mM $BaCl_2$ as shown on the top line, and perfused internally with solution containing either 0.3 or 3.0 mM $[Mg^{2+}]_i$ as shown on the second line. (*A*) Effect of internal $[Mg^{2+}]$ on amplitude of the inward current. Each square represents a current, which was evoked by a 400-ms pulse to 0 mV from −80 mV. The amplitude of the current was determined as the peak inward current minus the current obtained at 400 ms in response to an identical pulse in the presence of 2 mM $CdCl_2$ (+10 pA). At four times, marked *IV*, current-voltage relationships were determined by a series of 200-ms pulses to voltages between −50 and +50 mV. The small numbers *1–4* correspond to the times the current records in *C* were taken. (*B*) Effect of $[Mg^{2+}]_i$ on inactivation of inward current. The inactivation of the current was expressed as the amplitude of the current at 195 ms relative to the peak amplitude of the current. I_{Ca} decays 100% within 195 ms under all conditions. The decay of I_{Ba}, by contrast, is increased by elevating $[Mg^{2+}]_i$. (*C*) Tracings of currents recorded at the time labeled *1–4* in *A*. Horizontal line in this and subsequent figures indicates zero current. Each trace is 400 ms long. The gains in *1* and *4* are twice the gains in *2* and *3*. The amplitude of the traces are shown in *A*.

was changed from 3.0 to 0.3 mM $[Mg^{2+}]_i$, I_{Ba} or I_{Ca} increased up to 140% (see Fig. 2 *C* in White and Hartzell, 1988). The currents elicited by the routine test pulses to 0 mV accurately reflected the maximum current amplitude obtainable under each condition, as shown by the *I-V* curves determined under the four different conditions. These results on I_{Ca} are consistent with those we have published previously (White and Hartzell, 1988).

Increasing $[Mg^{2+}]_i$ altered the inactivation of I_{Ba} drastically, as shown in Fig. 1, *B* and *C*. As an imperfect measure of current inactivation, the amplitude of the current at 195 ms was expressed as a percentage of the maximum current. I_{Ca} decayed almost completely within 195 ms with both 0.3 and 3.0 mM $[Mg^{2+}]_i$. In contrast, with 0.3 mM $[Mg^{2+}]_i$, I_{Ba} decayed <10% in 195 ms, but changing $[Mg^{2+}]_i$ to 3.0 mM produced a marked increase in I_{Ba} decay. Currents obtained under these four conditions (numbered *1–4* in Fig. 1 *A*) are shown in Fig. 1 *C*. Despite the fact that these currents had an embarrassing amount of 60 Hz noise, it was clear that increasing $[Mg^{2+}]_i$ converted the very slowly inactivating I_{Ba} into a current that decayed almost

TABLE II

Effects of Magnesium on I_{Ca} and I_{Ba}

$[Mg^{2+}]_i$ (mM)	0.3	3.0	0.3	3.0
Charge carrier (*mM*)	1.8 Ca^{2+}	1.8 Ca^{2+}	2 Ba^{2+}	2 Ba^{2+}
Current density (*A/F*)	2.90 ± 0.34 (49)	2.44 ± 0.30 (13)	8.83 ± 1.10 (25)	5.68 ± 0.80 (25)
% Decay at 195 ms	103 ± 1.8 (50)	101 ± 1.4 (13)	56.8 ± 2.4 (45)	81.2 ± 2.1 (17)
Peak *I-V* (*mV*)	5 ± 1.3 (15)	−3 ± 1.7 (10)	4.1 ± 1.5 (12)	−5 ± 2.2 (6)
Half-inactivation (*mV*)	−24.3 ± 1.1 (15)	−30.8 ± 1.9 (10)	−19.8 ± 4.2 (12)	−27.5 ± 2.7 (6)
Availability at 0 mV*	0.04 ± 0.02 (8)	0.03 ± 0.04 (5)	0.51 ± 0.06 (13)	0.27 ± 0.04 (6)
Availability at 100 mV*	0.65 ± 0.04 (15)	0.29 ± 0.05 (10)	0.60 ± 0.04 (13)	0.41 ± 0.05 (6)
Steady-state availability‡			0.34 ± 0.05 (7)	0.15 ± 0.04 (4)

Data are mean ± SE (*N*).

*Availability is defined as $1 - (I_{test}/I_{control})$ in a two-pulse protocol with a 200-ms prepulse.

‡Steady-state availability is defined as $1 - (I_{test}/I_{control})$ in a two-pulse protocol with a 2- or 3-s prepulse to 0 mV.

as rapidly as I_{Ca}. The effect of high $[Mg^{2+}]_i$ on the amplitude and decay of I_{Ba} was at least partially reversible except after prolonged (>30 min) internal perfusion.

$[Mg^{2+}]_i$ influenced the *I-V* relationships for both I_{Ba} and I_{Ca} as shown in Fig. 2. The peaks of the *I-V* relationships were shifted ~5–10 mV in the negative direction upon changing from 0.3 to 3.0 mM $[Mg^{2+}]_i$ (see also Table II). The *I-V* relationships in high $[Mg^{2+}]_i$ were also skewed towards negative potentials. Furthermore, the reversal potential for the current was shifted towards negative potentials. It has been shown in these cells that I_{Ca} exhibits a true reversal potential and that the current in the outward direction is largely carried by K^+ (or in this case, Cs^+) (Campbell et al., 1988). This change in the reversal potential produced by internal Mg^{2+} could be due either to (*a*) Mg^{2+} carrying current in the outward direction through the Ca^{2+} channel or (*b*) Mg^{2+} increasing the ability of monovalent ions to move through the Ca channel in the outward direction.

Ca Channel Inactivation

Inactivation of I_{Ca} is considered to have a Ca-dependent and a voltage-dependent component, but the inactivation of I_{Ba} is primarily voltage dependent. Because elevating $[Mg^{2+}]_i$ accelerated the inactivation of I_{Ba}, we hypothesized that increasing $[Mg^{2+}]_i$ increased the voltage-dependent component of inactivation. Before examining the effects of $[Mg^{2+}]_i$ on inactivation, we wanted to characterize in more detail the inactivation of I_{Ca} and I_{Ba}. The rates of Ca-dependent and voltage-dependent inactivation were estimated by a standard two-pulse protocol consisting of a prepulse of varying duration and amplitude followed at a 3-ms interval by a 200-ms test

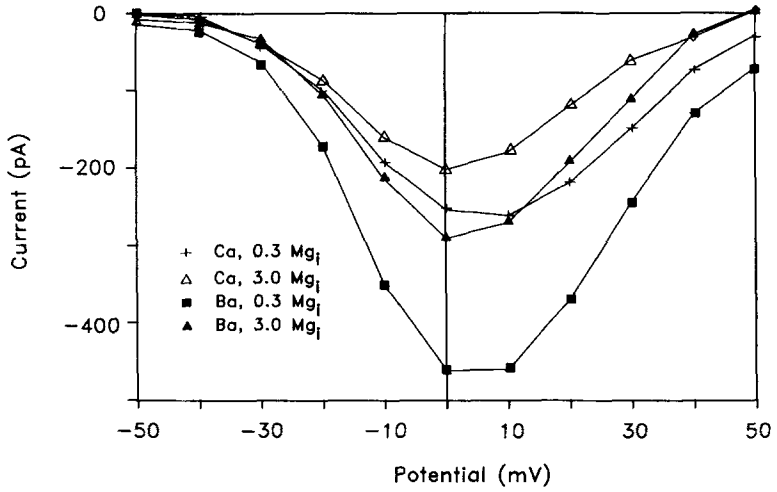

FIGURE 2. Current-voltage relationships of I_{Ca} and I_{Ba} with different $[Mg^{2+}]_i$. Current-voltage relationships were obtained by 200-ms pulses from −80 mV holding potential. Currents were leak-subtracted. (*Filled squares*) External solution: Ringers solution with 2 mM $BaCl_2$, 1.8 mM $MgCl_2$. Internal solution 0.3 mM $[Mg^{2+}]$. (*Filled triangles*) External solution: 2 mM $BaCl_2$, 1.8 mM $MgCl_2$. Internal solution: 3.0 mM $[Mg^{2+}]$. (*Pluses*) External solution: 1.8 mM $CaCl_2$, 1.8 mM $MgCl_2$. Internal solution: 0.3 mM $[Mg^{2+}]$. (*Triangles*) External solution: 1.8 mM $CaCl_2$, 1.8 mM $MgCl_2$. Internal solution: 3.0 mM $[Mg^{2+}]$.

pulse from −80 to 0 mV. The amplitude of I_{Ca} elicited by the test pulse was expressed as a percentage of I_{Ca} in the absence of a prepulse.

The inactivation curve for I_{Ca} had a characteristic "U"-shape (Fig. 3 *A*) as described previously by others (Tillotson, 1979; Eckert and Tillotson, 1981; Mentrard et al., 1984; Hadley and Hume, 1987; Argibay et al., 1988). Increasing inactivation of I_{Ca} occurred with prepulses between −60 and 0 mV, with maximum inactivation occurring as prepulses neared 0 mV. With prepulses of short duration, inactivation decreased as prepulses became positive to 0 mV. This decrease in inactivation has been called "relief from inactivation" (Lee et al., 1985) and is due to the fact that the inactivation curve with Ca^{2+} as charge carrier is the sum of voltage-dependent inactivation (which is incomplete especially with short duration prepulses) and calcium-dependent inactivation (which is greatest in magnitude around

0 mV). Fig. 3 *B* illustrates the inactivation curves obtained in the same cell using Ba^{2+} as charge carrier. Under these conditions, we assumed that only voltage-dependent inactivation was being measured. Under these conditions, the inactivation curve was much less U-shaped: it was sigmoidal with a plateau between 0 and +100 mV.

It was difficult to obtain a complete series of curves as shown in Fig. 3 from a single cell, because the cells often deteriorated during the long prepulses. Thus, we often measured the time course of inactivation produced by prepulses to 0 mV only. Fig. 4 *A* shows the time course of inactivation measured by a series of prepulses of

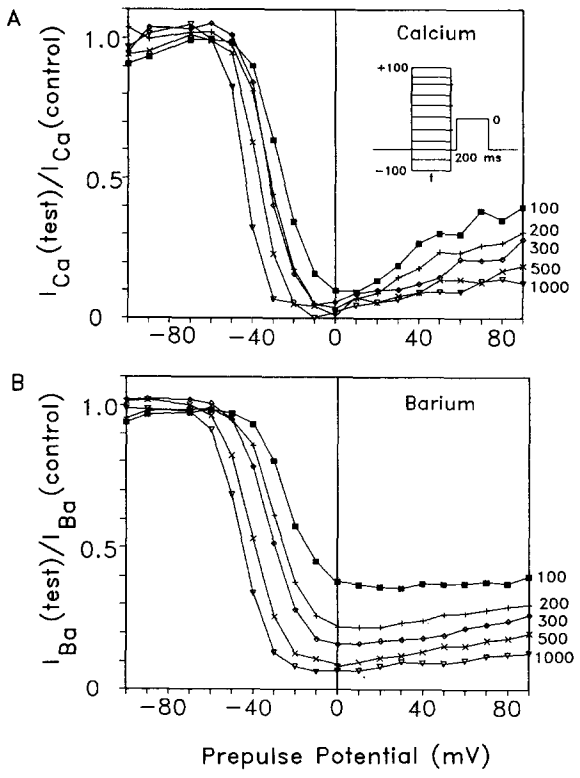

FIGURE 3. Time course of inactivation of I_{Ca} and I_{Ba}. (*A*) I_{Ca} inactivation. Internal solution contained 1.0 mM [Mg^{2+}]. External solution contained 1.8 mM $CaCl_2$, 1.8 mM $MgCl_2$. A two-pulse inactivation protocol consisted of a prepulse to the voltage indicated on the *x*-axis of duration 100-ms (*squares*), 200 ms (*pluses*), 300 ms (*diamonds*), 500 ms (*crosses*), or 1,000 ms (*inverted triangles*) followed after a 3-ms interval by a test pulse to 0 mV of 200 ms duration. The amplitude of the response to the test pulse preceded by a prepulse was plotted as a fraction of the amplitude of the response to the test pulse in the absence of a prepulse. (*B*) I_{Ba} inactivation from the same cell as in *A*. The solutions and conditions were the same as in *A* except that 2 mM $BaCl_2$ replaced 1.8 mM $CaCl_2$ in the external solution.

different durations to 0 mV. Voltage-dependent inactivation alone (barium curve) was relatively slower than inactivation produced by Ca-dependent and voltage-dependent processes together (calcium curve). With Ba^{2+} as charge carrier, 50% inactivation was produced by 60-ms prepulses, and steady-state inactivation was achieved with 700-ms prepulses. With Ca^{2+} as charge carrier, inactivation was at least twice as fast and was complete within 200 ms. The amount of Ca-dependent inactivation relative to the voltage-dependent component was calculated as the ratio of the difference between the two curves and the barium curve (Fig. 4 *B*). Ca-dependent inactivation contributed most to inactivation with short prepulses and then declined as the amount of voltage-dependent inactivation increased.

Effects of $[Mg^{2+}]_i$ on Inactivation

$[Mg^{2+}]_i$ has distinct effects on inactivation measured by the two-pulse protocol with 200-ms duration prepulses (Fig. 5). With Ca^{2+} as charge carrier, increasing $[Mg^{2+}]_i$ had two effects: it shifted half-inactivation ~5 mV in the negative direction (Table II), and it depressed relief from inactivation considerably. In Fig. 5, relief from inactivation with prepulses to +90 mV decreased from 90 to 30% as $[Mg^{2+}]_i$ was increased from 0.3 to 3.0 mM. On average, with Ca^{2+} as charge carrier, increasing $[Mg^{2+}]_i$ from 0.3 to 3.0 mM produced a 56% depression in relief from inactivation (Table II). With Ba^{2+} as charge carrier, half-inactivation was shifted 8 mV in a neg-

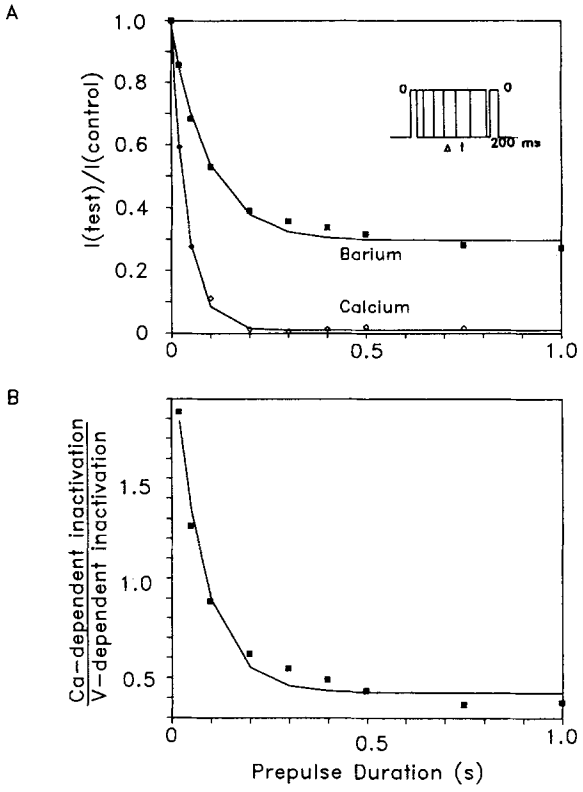

FIGURE 4. Time course of inactivation of I_{Ca} and I_{Ba} at 0 mV. A two-pulse protocol consisted of prepulses to 0 mV for the durations shown on the *x*-axis followed after a 3-ms interval (−80 mV) by a 200-ms test pulse to 0 mV. Inactivation was plotted as in Fig. 3. Solutions and conditions were the same as in Fig. 3. (*Squares*) 2 mM $BaCl_2$ in external solution. (*Diamonds*) 1.8 mM $CaCl_2$ in external solution. (*B*) Time course of Ca-dependent inactivation relative to voltage-dependent inactivation at 0 mV. Ca-dependent inactivation was defined as the difference between the inactivation curve in Ba^{2+} and in Ca^{2+}. Voltage-dependent inactivation was defined as the curve in Ba^{2+}. The ratio between Ca-dependent and voltage-dependent inactivation is plotted as a function of the prepulse duration.

ative direction, and the plateau of inactivation between 0 and +100 mV was diminished by >50% when $[Mg^{2+}]_i$ was increased.

Since the inactivation protocol with 200-ms prepulses did not produce steady-state inactivation of I_{Ba}, the difference in the inactivation curves with low and high $[Mg^{2+}]_i$ could have been caused by changes in the rate of inactivation or in the level of steady-state inactivation. Our results suggest that $[Mg^{2+}]$ may affect both of these variables, as shown in Fig. 6. The time course of inactivation was measured by examining the effect of different duration prepulses to 0 mV on the response to the standard test pulse to 0 mV (Fig. 6 *A*). Increasing $[Mg^{2+}]_i$ caused a dramatic increase

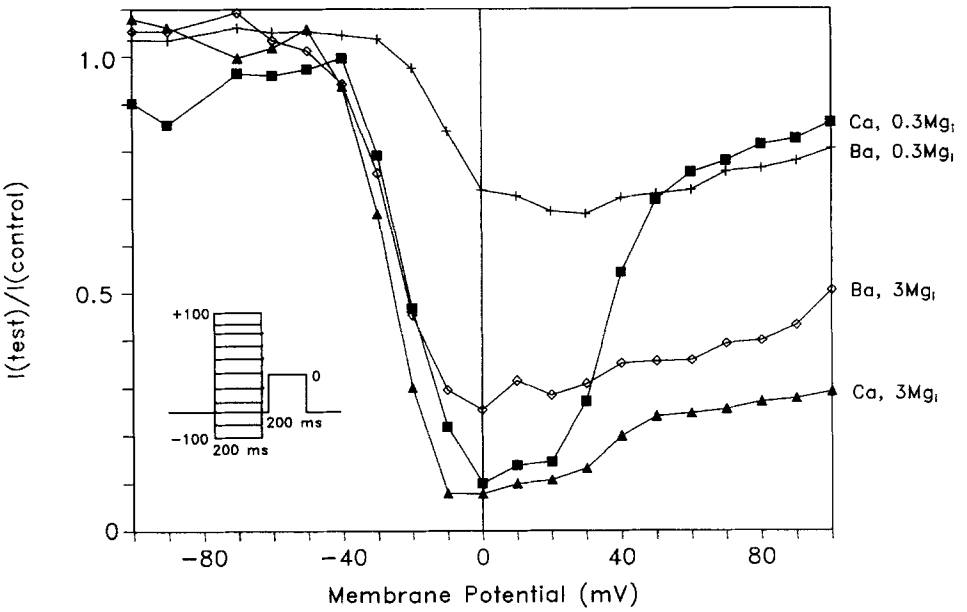

FIGURE 5. Effect of $[Mg^{2+}]_i$ on inactivation of I_{Ca} and I_{Ba}. Inactivation was measured as in Fig. 3 with 200-ms duration prepulses. These curves were determined in the same cell that was first perfused internally with a solution containing 0.3 mM $[Mg^{2+}]_i$ (*squares, pluses*), and then with a solution containing 3.0 mM $[Mg^{2+}]_i$ (*diamonds, triangles*). The cell was alternatively exposed to external solution containing 1.8 mM $CaCl_2$ (*squares, triangles*) or 2 mM $BaCl_2$ (*diamonds, pluses*). External $[Mg^{2+}]$ was 1.8 mM.

in the rate of inactivation and in the steady-state level of inactivation. The data in Fig. 6 *A* were fitted to single exponentials with time constants of 155 ms for 0.3 mM $[Mg^{2+}]_i$ and 69 ms for 3.0 mM $[Mg^{2+}]_i$. As stated above, it was difficult to measure a true steady-state inactivation in these cells due to the deterioration of the cells with long pulses. One of the few examples in which we were able to measure a quasi–steady-state inactivation curve in two different $[Mg^{2+}]_i$ concentrations is shown in Fig. 6 *B*. In this cell, I_{Ba} inactivation was measured with the two-pulse protocol using 3-s prepulses. When the cell was perfused with 3.0 mM $[Mg^{2+}]_i$, half-inactivation was shifted in the negative direction and the steady-state level of inactivation was considerably less. However, upon returning to 0.3 mM $[Mg^{2+}]_i$, the steady-state inactivation curve returned only slightly toward the initial 0.3 mM $[Mg^{2+}]_i$ curve. This lack

FIGURE 6. Effect of $[Mg^{2+}]_i$ on steady-state inactivation of I_{Ba}. (*A*) Time course of inactivation of I_{Ba} measured with a two-pulse protocol. Inactivation was determined as in Fig. 4 in the presence of either 0.3 or 3.0 mM $[Mg^{2+}]_i$. (*B*) Inactivation was determined as in Fig. 3 with 3-s duration prepulses. The cell was first perfused internally with 0.3 $[Mg^{2+}]_i$ (*squares*) followed by 3.0 mM $[Mg^{2+}]_i$ (*diamonds*) and a return to 0.3 mM $[Mg^{2+}]_i$ (*pluses*). (*C*) Normalized traces of Ba^{2+} currents obtained under the three conditions illustrated in *A*. These currents were obtained by pulses from −80 to 0 mV. The currents were normalized to the same net amplitude.

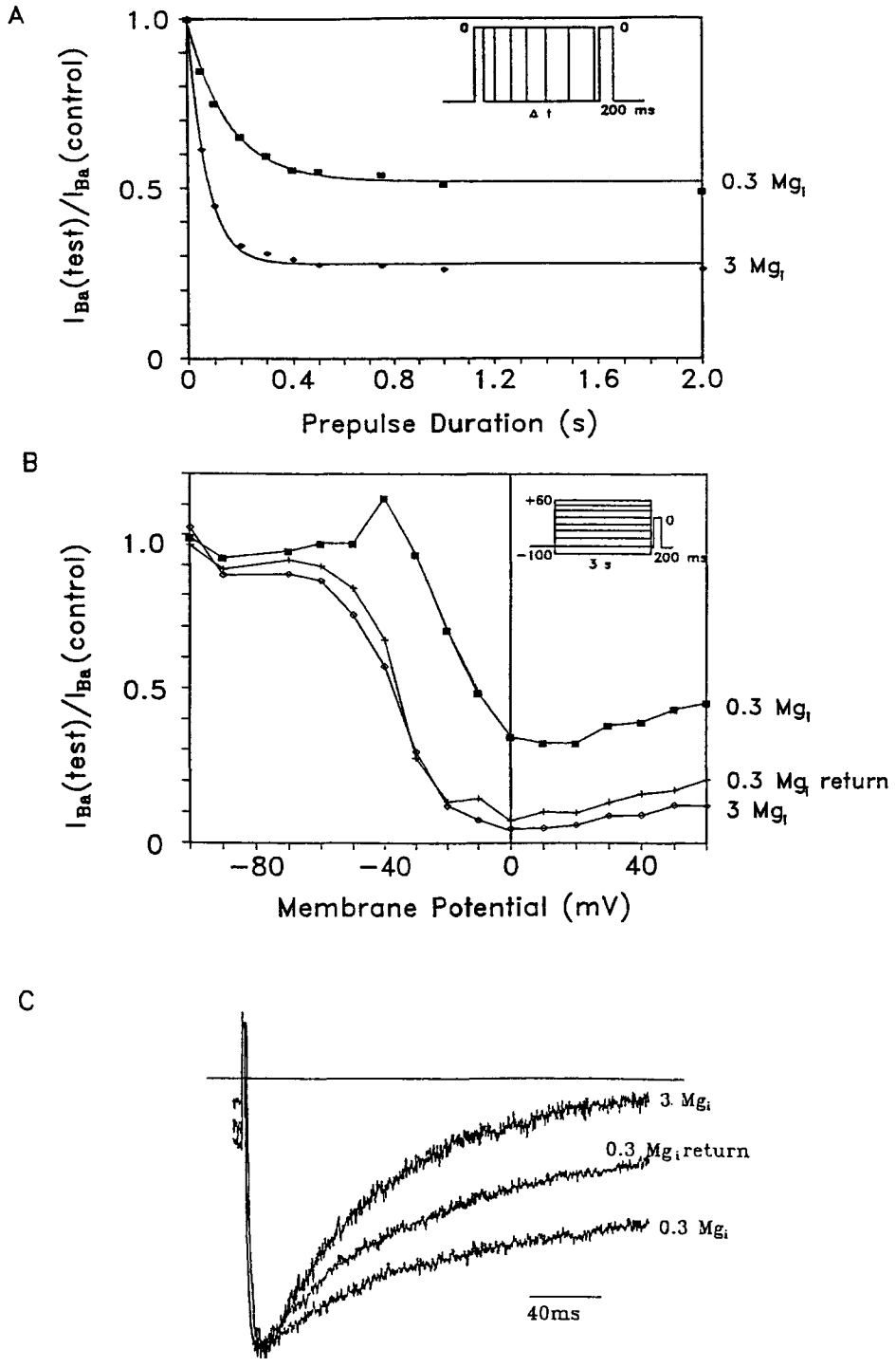
A
1.0
0.5
0
$I_{Ba}(test)/I_{Ba}(control)$
0
0.4
0.8
1.2
1.6
2.0
Prepulse Duration (s)
0
0
200 ms
Δ t
0.3 Mg_i
3 Mg_i
B
1.0
0.5
0
$I_{Ba}(test)/I_{Ba}(control)$
−80
−40
0
40
Membrane Potential (mV)
+60
0
−100
200 ms
3 s
0.3 Mg_i
0.3 Mg_i return
3 Mg_i
C
3 Mg_i
0.3 Mg_i return
0.3 Mg_i
40ms

FIGURE 6.

of reversibility of inactivation was commonly observed, and was always associated with deterioration of the cell: the holding current increased and the cell became rounded-up and swollen. Despite the fact that the steady-state inactivation curve was irreversibly affected by high $[Mg^{2+}]_i$, the kinetics of I_{Ba} inactivation were partly reversible (Fig. 6 *C*).

Voltage Dependence of Inactivation

The kinetics of inactivation of I_{Ba} were altered at all potentials. Fig. 7 *A* shows sample traces of I_{Ba} obtained at different test potentials with 0.3 and 3.0 mM $[Mg^{2+}]_i$. Examination of these traces shows that with 0.3 mM $[Mg^{2+}]_i$, inactivation of I_{Ba} was incomplete and the inactivating component of the current inactivated more slowly than with 3.0 mM $[Mg^{2+}]_i$. The potential dependence of inactivation is also evident in Fig. 7 *B*, where I_{Ba} and I_{200} are plotted. With 0.3 mM $[Mg^{2+}]_i$, I_{Ba} (solid squares) and I_{200} (solid triangles) were similar in amplitude for potentials negative to −20 mV. Increasing $[Mg^{2+}]_i$ to 3.0 mM greatly depressed I_{200} and shifted the peak of the I_{200} curve 10 mV in the negative direction. A quantitative analysis of the kinetics of inactivation is shown in Fig. 7 *C*. The currents were leak-subtracted and fitted to the sum of two exponentials plus an offset $[I_{Ba} = A * \exp(-t/\tau_2) + B * \exp(-t/\tau_2) + C]$. Each panel is a three-dimensional plot showing the amplitude (*A*, *B*, and *C*) (*z*-axis) and the time constant (τ_1 and τ_2) (*y*-axis) of each component as a function of test potential. Arbitrarily, the fast component was defined as having a time constant of <100 ms. The most noticeable difference between the currents obtained in 0.3 and 3.0 mM $[Mg^{2+}]_i$ was the difference in the relative magnitude of the offset. The offset was severalfold larger at almost every potential in 0.3 mM than it was in 3.0 mM $[Mg^{2+}]_i$. The rapidly inactivating component was the major component with 3.0 mM $[Mg^{2+}]_i$ at all voltages, but with 0.3 mM $[Mg^{2+}]_i$ the rapidly inactivating component was a minor component between +5 and −10 mV and was negligible at all other potentials. The fast time constant was similar with both 0.3 and 3.0 mM $[Mg^{2+}]_i$ (between 30 and 60 ms), but the slow time constant was considerably slower in 0.3 mM $[Mg^{2+}]_i$ than in 3.0 mM $[Mg^{2+}]_i$. Thus, these data show that increasing $[Mg^{2+}]_i$ decreased the relative magnitude of the noninactivating component of I_{Ba}, and decreased the time constant and decreased the amplitude of the slow component at all potentials.

These results suggest that a component of the "voltage-dependent" inactivation is increased by $[Mg^{2+}]_i$. To test whether voltage-dependent inactivation was due entirely to a Mg^{2+}-dependent mechanism, we examined the kinetics of I_{Ba} in cells perfused internally and superfused with solutions that were Mg^{2+} free (Fig. 8). The internal solution was similar to the 0.3 mM Mg^{2+} solution shown in Table I except that $MgCl_2$ and ATP were omitted and EDTA and BAPTA were added (see figure legends). I_{Ba} under these conditions had a time course that was slower than that observed with 0.3 mM $[Mg^{2+}]_i$, but the current still exhibited both an inactivating component and a noninactivating component. Thus, voltage-dependent inactivation cannot be caused entirely by a Mg^{2+}-dependent mechanism. Upon changing to 4.0 mM $[Mg^{2+}]_i$, I_{Ba} decreased in amplitude approximately 10-fold. I_{Ba} recorded in the presence of 4.0 mM $[Mg^{2+}]_i$ was much faster: the noninactivating component was markedly reduced and the slowly inactivating component was largely absent (Fig. 8).

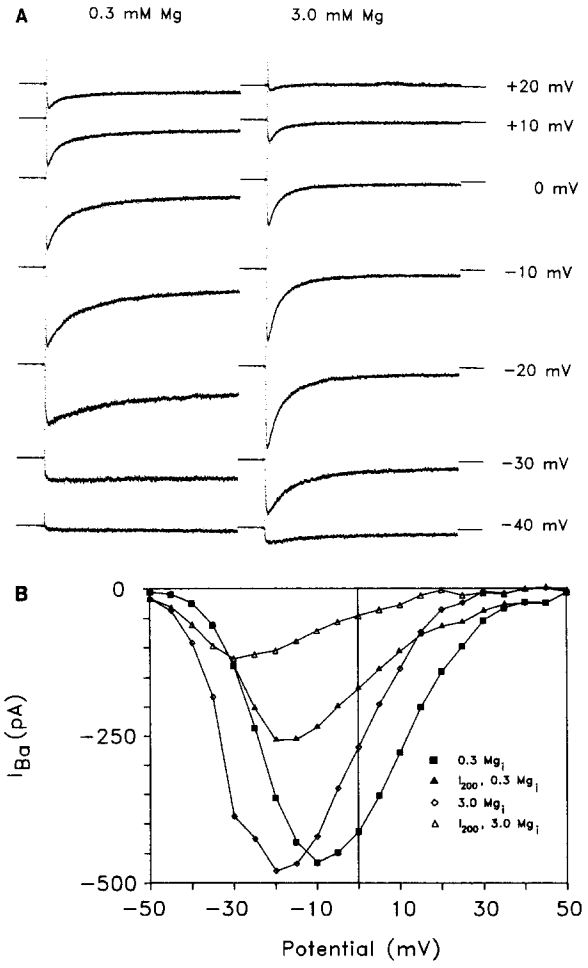

FIGURE 7. Effects of $[Mg^{2+}]_i$ on kinetics of inactivation of I_{Ba} at different potentials. I_{Ba} was evoked by 800-ms duration pulses from −80 mV to the potential indicated. Traces were leak-subtracted. External $[Mg^{2+}]$ was 0 mM. (*A*) Sample leak-subtracted current traces obtained at the voltages shown from the same cell perfused internally with either 0.3 mM $[Mg^{2+}]_i$ or 3.0 mM $[Mg^{2+}]_i$. (*B*) Current-voltage relationships for I_{Ba} in the same cell. (*Solid squares*) Leak-subtracted peak I_{Ba} amplitude with 0.3 mM $[Mg^{2+}]_i$. (*Solid triangles*) Amplitude of I_{Ba} at 200 ms after onset of pulse with 0.3 mM $[Mg^{2+}]_i$. (*Open diamonds*) Leak-subtracted peak I_{Ba} amplitude with 3 mM $[Mg^{2+}]_i$. (*Open triangles*) Amplitude of I_{Ba} at 200 ms with 3 mM $[Mg^{2+}]_i$. (*C*) Time constants of fits of I_{Ba}. Inactivation of Ba^{2+} currents were fit to the sum of two exponentials plus an offset $[(I_t = A^* \exp(-t/\tau_1) + B^* \exp(-t/\tau_2) + C]$. The amplitudes ($A$, B, and C) were normalized as a fraction of the largest amplitude component recorded for each $[Mg^{2+}]$ (this was the slow component at −15 mV for 0.3 mM $[Mg^{2+}]_i$ and the fast component at −15 mV for 3.0 mM $[Mg^{2+}]_i$. The amplitude (z-axis) and the time constant (y-axis) of each component are plotted as a function of the test pulse voltage.

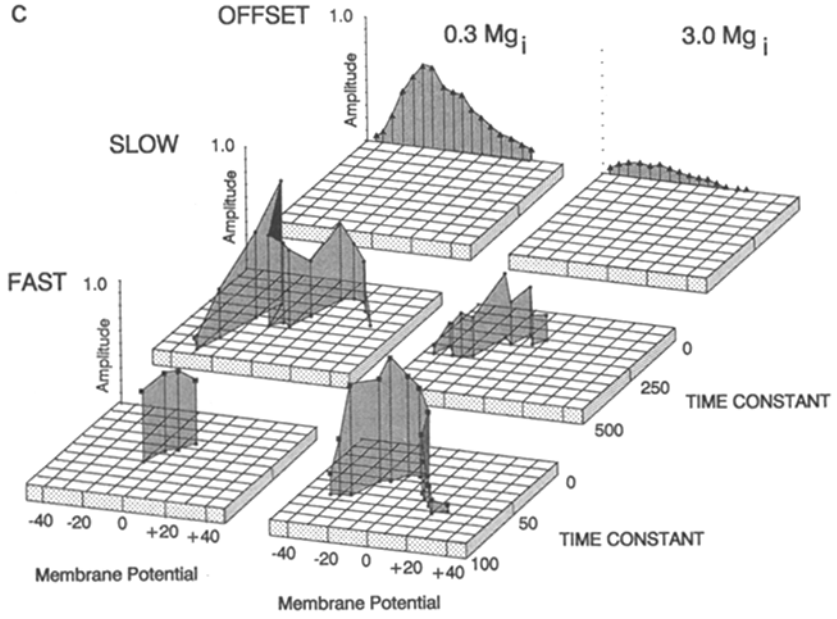

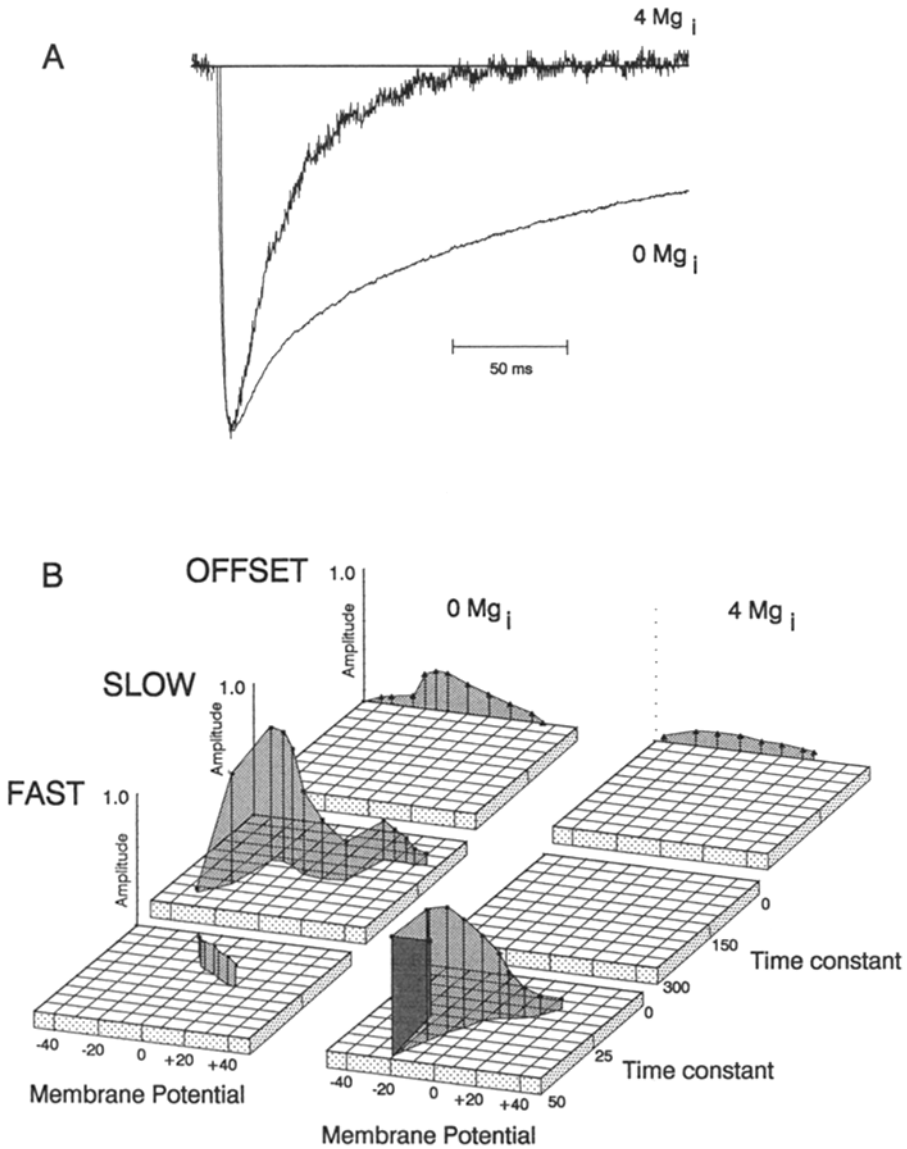

FIGURE 8. Effect of zero $[Mg^{2+}]_i$ and $[Mg^{2+}]_o$ on I_{Ba}. (*A*) Sample traces obtained by pulses from −80 to 0 mV in 0 mM $[Mg^{2+}]_i$ and 4.0 mM $[Mg^{2+}]_i$. The trace obtained with 4.0 mM $[Mg^{2+}]_i$ (107 pA) has been normalized to the same amplitude of the trace obtained under 0 mM $[Mg^{2+}]_i$ conditions (1,484 pA). (*B*) Plots of the time constants of fits of I_{Ba} to two exponentials plus an offset as described in Fig. 7. The composition of the internal 0 mM Mg^{2+} solution was (in millimolar): 102 CsCl, 10 K.PIPES, 10 CsEGTA, 5 Cs_2EDTA, 1 BAPTA, 5 Na_2creatinine phosphate, pH 7.15. The composition of the internal 4.0 mM Mg^{2+} solution was (in millimolar): 57.9 CsCl, 10 K.PIPES, 10 CsEGTA, 5 Cs_2EDTA, 1 BAPTA, 14.9 $MgCl_2$, 5 Na_2creatine phosphate, pH 7.15.

Thus, it appears that the characteristics of the current observed in 4.0 mM $[Mg^{2+}]_i$ depend to some extent upon the concentration of $[Mg^{2+}]_i$ to which the cell has been previously exposed.

These observations and the irreversible effect of high $[Mg^{2+}]_i$ raised the possibility that the change in kinetics might be due to a buildup of internal $[Ca^{2+}]_i$ in the presence of $[Mg^{2+}]_i$. A buildup of internal Ca^{2+} seems unlikely, however, because internal Ca^{2+} should be well buffered by the 10 mM EGTA, 5 mM EDTA, and 1 mM BAPTA in the internal solution (Fig. 8).

Effects of Holding Potential and Nifedipine

The ability of $[Mg^{2+}]_i$ to convert a slowly inactivating current to a rapidly inactivating one suggested the possibility that $[Mg^{2+}]_i$ was converting or altering the expression of T- and L-type Ca channels (Bean, 1985): high $[Mg^{2+}]_i$ might favor the expression of T channels. However, this hypothesis did not explain the results. With 0.3 $[Mg^{2+}]_i$ (Fig. 9 *A*), where I_{Ba} inactivated slowly, current-voltage relationships of I_{Ba} from holding potentials of -100 and -40 mV, and the difference between these curves, were virtually identical in shape and all had peaks near 0 mV. I_{Ba} was completely blocked by 0.1–1.0 μM nifedipine at holding potentials positive to -50 mV, and was blocked 80% at a holding potential of -100 mV (Fig. 9 *A*). This incomplete block was most likely due to the voltage-dependent nature of nifedipine block (Kass and Krafte, 1987). With 3.0 mM $[Mg^{2+}]_i$ (Fig. 9 *B*), I_{Ba} was almost completely inactivated at a holding potential of -40 mV. The current-voltage relationship from a holding potential of -50 mV, however, had the same shape as the current-voltage relationship obtained from -100 mV holding potential. I_{Ba} was completely blocked

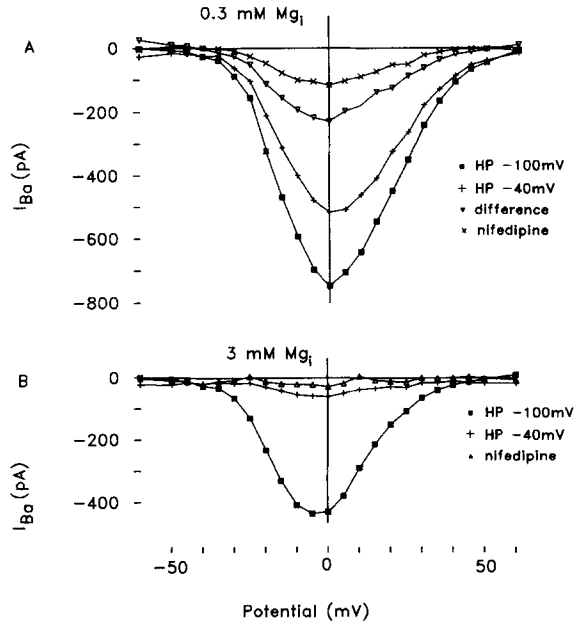

FIGURE 9. Absence of T-type Ca channels in frog ventricular cells. (*A*) Current-voltage relationships obtained in 0.3 $[Mg^{2+}]_i$ from holding potentials of -100 mV (*squares*) and -40 mV (*pluses*). The difference between these curves is shown as inverted triangles. The current-voltage relationship obtained in the presence of 1.0 μM nifedipine with a -100 mV holding potential is shown as crosses. (*B*) Current-voltage relationships obtained in 3.0 mM $[Mg^{2+}]_i$ under the same conditions.

by 1.0 μM nifedipine even from a holding potential of −100 mV under these conditions. Thus, there was no evidence for T-type Ca channels in this preparation.

Effects of External [Mg^{2+}] on I_{Ca} and I_{Ba}

External Mg^{2+} has been shown previously by other investigators to block Ca channels. Thus, we wished to compare the effects of external and internal [Mg^{2+}] on I_{Ba}. As shown in Fig. 10, $[Mg^{2+}]_i$ and $[Mg^{2+}]_o$ were varied between 0.3 and 3.0 mM and the effects on I_{Ba} measured. The kinetics of leak-subtracted currents were quantified by fitting them to the sum of two exponentials using the program FIT. In this cell, raising $[Mg^{2+}]_i$ from 0.3 to 3.0 mM decreased the amplitude of I_{Ba} by ~55% regardless of $[Mg^{2+}]_o$ (either 0.3 or 3.0 mM). Raising $[Mg^{2+}]_o$ caused a decrease in I_{Ba}

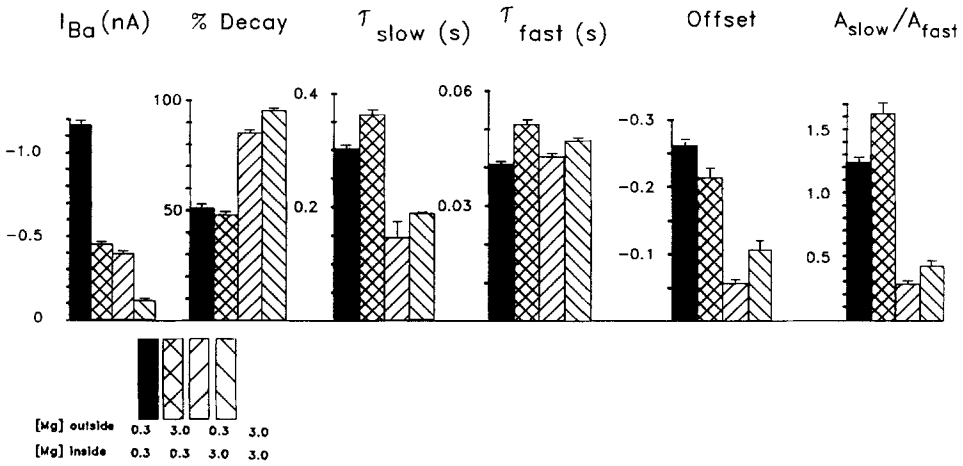

FIGURE 10. Effects of internal and external [Mg^{2+}] on I_{Ba}. I_{Ba} was elicited by 800-ms duration pulses from −80 to 0 mV in the presence of 0.3 or 3.0 mM $[Mg^{2+}]_i$ and 0.3 or 3.0 mM $[Mg^{2+}]_o$. At least seven currents were recorded in each condition, leak-subtracted, and fitted to the sum of two exponentials. The bar graphs illustrate I_{Ba} amplitude, percent decay (as described in Fig. 1), the best fit time constants (τ_{slow} and τ_{fast}), the ratio between the amplitudes of the rapidly and slowly inactivating components (A_{slow}/A_{fast}), and the amplitude of the noninactivating component (C).

amplitude that was similar in magnitude to the effect of raising $[Mg^{2+}]_i$. Changing $[Mg^{2+}]_o$ had no significant effect on the inactivation of I_{Ba}. The percent decay (at 195 ms) approximately doubled when $[Mg^{2+}]_i$ was increased from 0.3 to 3.0 mM. Altering $[Mg^{2+}]_o$ had little effect upon I_{Ba} decay, regardless of whether the cell was internally perfused with 0.3 or 3.0 mM $[Mg^{2+}]_i$. Changing internal or external [Mg^{2+}] had minimal effects on the fast component of inactivation, but increasing $[Mg^{2+}]_i$ decreased the time constant and the amplitude of the slow component of inactivation and decreased the offset. Increasing external [Mg^{2+}] had effects that were qualitatively opposite to that of increasing $[Mg^{2+}]_i$ on the kinetics of inactivation, except that these effects were relatively small. Specifically, increasing $[Mg^{2+}]_o$ increased the time constant and amplitude of the slow component of inactivation and may have increased the offset when 3 mm Mg^{2+} was present inside.

The difference in the effect of $[Mg^{2+}]_i$ and $[Mg^{2+}]_o$ on inactivation is further illustrated in Fig. 11 (compare with Fig. 5). Changing $[Mg^{2+}]_o$ from 0 to 5.0 mM shifts the 200-ms inactivation curve in a manner consistent with charge screening produced by $[Mg^{2+}]_o$ (Kass and Kraft, 1987). There is relatively little effect of external $[Mg^{2+}]$, however, on the relief from inactivation.

DISCUSSION

I_{Ca} plays a key role in the development of the action potential (Reuter, 1983; Tsien, 1983; Trautwein and Pelzer, 1985), in the generation of electrical pacemaking in nodal tissue (Noma et al., 1980), and in the initiation of contraction (Beeler and Reuter, 1970; Vassort and Rougier, 1972). I_{Ca} is modulated by cAMP-dependent

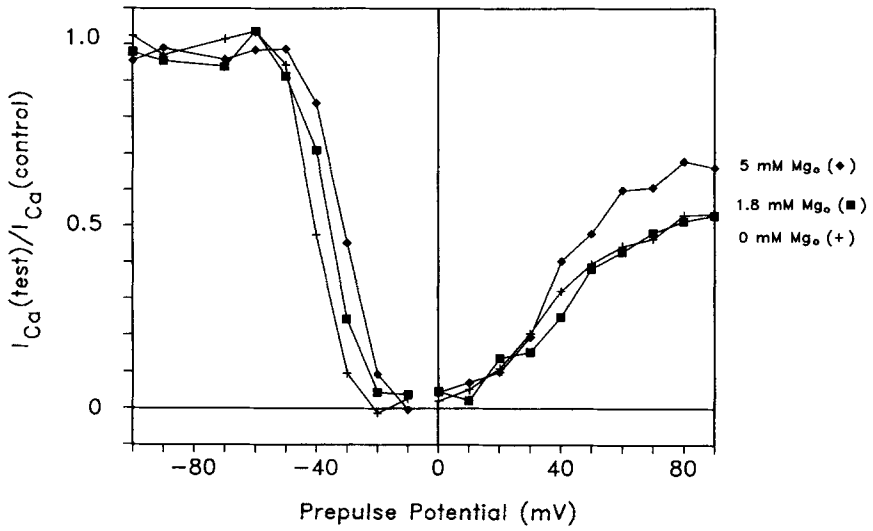

FIGURE 11. Effect of external $[Mg^{2+}]$ on I_{Ca} inactivation. Inactivation was measured by the standard two-pulse protocol with 200-ms prepulses. The cell was perfused internally with 0.3 mM $[Mg^{2+}]_i$ and superfused with solution containing either 5 mM $[Mg^{2+}]_o$ (*diamonds*), 1.8 mM $[Mg^{2+}]_o$ (*squares*), or 0 $[Mg^{2+}]_o$ (*pluses*).

protein phosphorylation by neurotransmitters and drugs that influence β-adrenergic and cholinergic receptors on cardiac cells (Tsien, 1977; Reuter, 1983; Trautwein and Pelzer, 1985; Fischmeister and Hartzell, 1986; Tsien et al., 1986; Hartzell and Fischmeister, 1987; Hartzell, 1989).

We found previously that increasing $[Mg^{2+}]_i$ had only small effects on basal I_{Ca} amplitude, but caused large decreases in I_{Ca} elevated by cAMP-dependent processes (White and Hartzell, 1988). We have argued that this effect is on a process that occurs after Ca channel phosphorylation, because the effect of $[Mg^{2+}]_i$ is seen under conditions that would not be expected to alter Ca channel phosphorylation. In this study we have confirmed that $[Mg^{2+}]_i$ has little effect on the amplitude of basal I_{Ca}, but we have found that Mg_i^{2+} has large effects on I_{Ba} amplitude and inactivation even when the channel is not phosphorylated. The effects of $[Mg^{2+}]_i$ on inactivation

were quite similar for I_{Ba} under basal or cAMP-stimulated conditions (data not shown). It is not clear whether the decrease in I_{Ba} amplitude produced by increasing $[Mg^{2+}]_i$ is related to the more rapid inactivation under these conditions or whether different mechanisms mediate the effects of $[Mg^{2+}]_i$ on inactivation and amplitude.

The apparent shift in reversal potential of I_{Ca} that is produced by $[Mg^{2+}]_i$ is somewhat curious. These results suggest either that Mg^{2+} may permeate Ca channels or that Mg^{2+} increases the permeability of the channel to monovalent ions such as Cs^+. Further studies are definitely warranted to investigate this point.

$[Mg^{2+}]_i$ Affects Inactivation

In heart, it appears that I_{Ca} inactivation is controlled by two mechanisms, one voltage dependent and the other calcium dependent (Eckert and Chad, 1984; Kass and Sanguinetti, 1984; Bechem and Pott, 1985; Lee et al., 1985; Chad and Eckert, 1986; Kass et al., 1986). Some laboratories, however, have proposed that I_{Ca} inactivation is due entirely to a Ca-dependent mechanism at least in snail neurons and GH_3 cells (Tillotson, 1979; Eckert and Tillotson, 1981; Chad and Eckert, 1986), but other laboratories find only voltage-dependent inactivation (for example, Cohen and Lederer, 1987). Both mechanisms clearly exist, but their proportion may depend upon experimental conditions and the tissue studied. The existence of a Ca-dependent mechanism is supported by the observations that inactivation increases with increasing intracellular or extracellular $[Ca^{2+}]$, that it is greatly slowed when ions other than Ca^{2+} (such as Ba^{2+}) are used as charge carrier, reduced when intracellular Ca^{2+} is chelated, and slowed when the driving force for Ca^{2+} entry is reduced (Eckert and Chad, 1984; Kass et al., 1986). The existence of "pure" voltage-dependent inactivation has been demonstrated by a two-pulse protocol in which the prepulse is given in the absence of Ca^{2+} (Akaike et al., 1988) or by using Na^+ as charge carrier (Hadley and Hume, 1987). The kinetics of I_{Ca} inactivation suggest that the rapid phase of inactivation is due to the Ca-dependent component, whereas the slow component is voltage dependent.

The "U"-shape of the inactivation curve (Fig. 3) can be viewed as the sum of the voltage-dependent inactivation, which can be described by a Boltzman relation with incomplete inactivation (Fig. 3 *B*), and the calcium-dependent inactivation, which has the same shape as the I_{Ca} current-voltage relationship. Our data in Fig. 3 show that for short-duration prepulses Ca-dependent inactivation predominates, whereas for longer-duration prepulses voltage-dependent inactivation predominates. It may be for this reason that some investigators (for example, Cohen and Lederer, 1987) fail to find clear evidence of Ca-dependent inactivation under conditions of steady-state inactivation. Below, we propose that voltage-dependent inactivation is actually due, at least partially, to a voltage- and time-dependent block of Ca^{2+} channels by Mg^{2+}.

With either Ca^{2+} or Ba^{2+} as charge carrier, increasing $[Mg^{2+}]_i$ shifts the inactivation curve to the left and decreases relief from inactivation (the decrease in inactivation with prepulses positive to 0 mV). The shift in the inactivation curve is most likely due to the ability of Mg^{2+} to screen negative surface charges on the internal surface of the membrane. Changes in external divalent ion concentrations produce

shifts in current-voltage relationships and inactivation curves that reflect divalent cations binding to and screening negatively charged groups (sialic acid groups, primarily) on the cell surface (Frankenhaeuser and Hodgkin, 1957; Kass and Kraft, 1987). In heart cells, a 10-fold change in external $[Ca^{2+}]$ shifts the inactivation curve ~30 mV, whereas a 10-fold change in external $[Mg^{2+}]$ shifts the curve only ~10 mV due to the lower affinity of $[Mg^{2+}]_i$ for the surface charges (Kass and Kraft, 1987). The shift in the inactivation curve is similar in magnitude, but opposite in direction for the same changes in $[Mg^{2+}]_o$ and $[Mg^{2+}]_i$. That is, a 10-fold increase in $[Mg^{2+}]_i$ shifts the current-voltage relationships and the inactivation curves ~10 mV to the left, whereas a 10-fold increase in $[Mg^{2+}]_o$ shifts the curves 10 mV to the right. This suggests that internal surface charge is similar in magnitude to external surface charge. This might be expected considering the asymmetrical distribution of phospholipids in the plasma membrane: negatively charged phosphatidyl serines are often concentrated in the internal leaflet of the lipid bilayer. In addition, negative internal surface charge may be partly due to the phosphate groups on phosphorylation sites on cytoplasmic domains of membrane proteins.

Although surface charge effects can explain the shifts in the inactivation and *I-V* curves, they are unlikely to explain the changes in relief from inactivation. Relief from inactivation observed with Ca^{2+} as charge carrier is largely an expression of the fact that voltage-dependent inactivation is incomplete at voltages positive to 0 mV with low $[Mg^{2+}]_i$. The incomplete nature of voltage-dependent inactivation is demonstrated by the plateau of the steady-state inactivation curves with Ba^{2+} as charge carrier and by the incomplete inactivation of I_{Ba} at most potentials. The incomplete inactivation of I_{Ba} with low $[Mg^{2+}]_i$ is not simply due to a shift in the inactivation parameters as a function of voltage, as would be expected from changes in surface charge. Rather, $[Mg^{2+}]_i$ seems to affect the amount of voltage-dependent inactivation at all voltages. Relief from inactivation is decreased by cAMP (Argibay et al., 1988) in a manner similar to that produced by increasing $[Mg^{2+}]_i$. It is worth considering that this decrease in relief from inactivation produced by cAMP might be related to accumulation of $[Mg^{2+}]_i$ due to rapid hydrolysis of ATP for protein phosphorylation.

With Ca^{2+} as charge carrier, increasing $[Mg^{2+}]_i$ does not have a significant effect on the kinetics of I_{Ca} inactivation as it does when Ba^{2+} is charge carrier. Thus, the effects of $[Mg^{2+}]_i$ are evident only when Ca^{2+}-dependent inactivation is suppressed. This suggests that $[Mg^{2+}]_i$ either affects mainly the voltage-dependent component of inactivation, or that $[Mg^{2+}]_i$ is capable of stimulating the Ca^{2+}-dependent inactivation process in the absence of Ca^{2+}. The effect of $[Mg^{2+}]_i$ on I_{Ba} inactivation appears to be due to an increase in both the rate and the steady-state level of voltage-dependent inactivation.

One explanation for the accelerated inactivation induced by internal Mg^{2+} was that $[Mg^{2+}]_i$ might stimulate Ca^{2+}-dependent inactivation. The data do not obviously support this hypothesis, however. We have previously reported that I_{Ca} inactivation is fit by the sum of two exponentials with time constants of ~13 ms and ~30 ms (Argibay et al., 1988). Replacement of Ca^{2+} with Ba^{2+} results in the 13-ms component of inactivation slowing to 240 ms (Argibay et al., 1988). Thus, one could conclude that the 30-ms component represents voltage-dependent inactivation and the

13-ms component represents Ca^{2+}-dependent inactivation. Since increasing $[Mg^{2+}]_i$ did not result in the addition of a ~13-ms component to I_{Ba} inactivation, but rather caused a decrease in the relative contribution of the noninactivating component and slowly inactivating components, this suggests that $[Mg^{2+}]_i$ is not mimicking the Ca^{2+}-dependent inactivation. It is possible that inhibition of I_{Ba} by internal Mg^{2+} is due to Mg^{2+} block subsequent to its partial entry into the channel from the cytoplasmic side or to interaction with some allosteric site on the channel.

Since the relative contribution of the "30-ms" voltage-dependent component increases with increasing $[Mg^{2+}]_i$, one could conclude that voltage-dependent inactivation is dependent upon $[Mg^{2+}]_i$. An obvious prediction of this hypothesis is that voltage-dependent inactivation should be eliminated when $[Mg^{2+}]_i$ is zero. Under these conditions, I_{Ba} continued to exhibit a "30-ms" inactivating component. Thus, it appears that voltage-dependent inactivation is not absolutely magnesium dependent. In support of this suggestion is the observation that voltage-dependent inactivation of cardiac muscle L-type channels incorporated into bilayers exhibit voltage-dependent inactivation in the absence of internal and external Mg^{2+} (Rosenberg et al., 1988). Nevertheless, we propose that a component of voltage-dependent inactivation is stimulated by $[Mg^{2+}]_i$. Further experimentation will be required to resolve these questions.

Varieties of Ca^{2+} Channels in Frog Ventricular Cells

Other investigators have reported that cardiac cells have multiple kinds of Ca^{2+} channels that can be distinguished on the basis of their inactivation properties and sensitivity to dihydropyridines (Bean, 1985; Nilius et al., 1985; Mitra and Morad, 1986). T-type channels have a peak *I-V* relationship near −20 mV, and are inactivated by a holding potential of −40 mV, whereas L-type channels have a peak *I-V* relationship positive to 0 mV, and are not inactivated appreciably at 40 mV holding potential. L-type channels inactivate slowly with Ba^{2+} as charge carrier, whereas T-type channels inactivate quickly. We have previously reported that frog ventricular cells have only L-type Ca^{2+} channels (Argibay et al., 1988), but this conclusion was based largely on studies with Ca^{2+} as charge carrier and with 1.0 mM $[Mg^{2+}]_i$. The rapid inactivation of I_{Ba} with 3.0 mM $[Mg^{2+}]_i$, however, suggested the possibility that $[Mg^{2+}]_i$ was inducing T-type channels in our preparation. We find no evidence, however, that this is the case. Current-voltage relationships, inactivation curves, and sensitivity to dihydropyridines all support the conclusion that there is only one kind of Ca channel, an L type.

Significance

It has been pointed out by Lee et al. (1985) that voltage-dependent inactivation of Ca^{2+} channels may be an important mechanism of Ca channel inactivation during an action potential, because the Ca^{2+} transient lags considerably behind the Ca^{2+} current and, consequently, Ca^{2+}-dependent inactivation might be small under these conditions. If this is true, changes in $[Mg^{2+}]_i$ that could occur physiologically might have significant effects on Ca^{2+} currents during the action potential. It is known that $[Mg^{2+}]_o$ alters action potential shape (Watanabe and Dreyfus, 1972; Chesnais et al., 1975), but it is not yet known what effects $[Mg^{2+}]_i$ has on the cardiac action

potential. Additional studies are required to determine whether $[Mg^{2+}]_i$ is physiologically regulated in cardiac cells and, if so, what effects this has on cardiac physiology (White and Hartzell, 1989).

We thank Drs. Rodolphe Fischmeister, David Armstrong, Eduardo Marban, Seiko Kawano, Armando Lagrutta, and Isabelle Gourdon for helpful comments and discussion and Dr. Robert Godt and Dr. Alexandre Fabiato for computer programs for calculating free ion composition of solutions.

Supported by grants HL-21195 and HL-21398 from the National Institutes of Health.

Original version received 25 July 1988 and accepted version received 17 April 1989.

REFERENCES

Akaike, N., Y. Tsuda, and Y. Oyama. 1988. Separation of current- and voltage-dependent inactivation of calcium current in frog sensory neuron. *Neuroscience Letters.* 84:46–50.

Alvarez-Leefmans, F. J., S. M. Gamino, F. Giraldez, and H. Gonzalez-Serratos. 1986. Intracellular free magnesium in frog skeletal muscle fibres measured with ion-selective micro-electrodes. *Journal of Physiology.* 378:461–483.

Argibay, J. A., R. Fischmeister, and H. C. Hartzell. 1988. Inactivation, reactivation and pacing dependence of calcium current in frog cardiocytes: Correlation with current density. *Journal of Physiology.* 401:201–226.

Bean, B. P. 1985. Two kinds of calcium channels in canine atrial cells. *Journal of General Physiology.* 86:1–30.

Bechem, M., and L. Pott. 1985. Removal of Ca current inactivation in dialysed guinea-pig atrial cardioballs by Ca chelators. *Pflügers Archives.* 404:10–20.

Beeler, G. W., and H. Reuter. 1970. Membrane calcium current in ventricular myocardial fibres. *Journal of Physiology.* 207:191–210.

Brown, A. M., K. Morimoto, Y. Tsuda, and D. L. Wilson. 1981. Calcium current-dependent and voltage-dependent inactivation of calcium channels in *Helix aspersa*. *Journal of Physiology.* 320:193–218.

Campbell, D. L., W. R. Giles, J. R. Hume, D. Noble, and E. F. Shibata. 1988. Reversal potential of the calcium current in bull-frog atrial myocytes. *Journal of Physiology.* 403:267–286.

Cech, S. Y., W. C. Broaddus, and M. E. Maguire. 1980. Adenylate cyclase: the role of magnesium and other divalent cations. *Molecular and Cellular Biology.* 33:67–92.

Chad, J. E., and R. Eckert. 1986. An enzymatic mechanism for calcium current inactivation in dialysed *Helix* neurones. *Journal of Physiology.* 378:31–51.

Chesnais, J. M., E. Coraboeuf, M. P. Sauviat, and J. M. Vassas. 1975. Sensitivity to H, Li, and Mg ions of the slow inward sodium current in frog atrial fibres. *Journal of Molecular and Cellular Cardiology.* 7:627–642.

Cohen, N. M., and W. J. Lederer. 1987. Calcium current in isolated neonatal rat ventricular myocytes. *Journal of Physiology.* 391:169–191.

Eckert, R., and J. E. Chad. 1984. Inactivation of Ca channels. *Progress in Biophysics and Molecular Biology.* 44:215–267.

Eckert, R., and D. L. Tillotson. 1981. Calcium-mediated inactivation of the calcium conductance in caesium-loaded giant neurones of *Apylsia californica*. *Journal of Physiology.* 314:265–280.

Fabiato, A. 1988. Computer programs for calculating total from free or free from specified total ionic concentrations in aqueous solution containing multiple metals and ligands. *Methods in Enzymology, Biomembranes.* 157:378–417.

Fischmeister, R., and H. C. Hartzell. 1986. Mechanism of action of acetylcholine on calcium current in single cells from frog ventricle. *Journal of Physiology.* 376:183–202.

Fischmeister, R., and H. C. Hartzell. 1987. Cyclic guanosine 3',5'-monophosphate regulates the calcium current in single cells from frog ventricle. *Journal of Physiology.* 387:453–472.

Flatman, P. W. 1984. Magnesium transport across cell membranes. *Journal of Membrane Biology.* 80:1–14.

Frankenhaeuser, B., and A. L. Hodgkin. 1957. The action of calcium on the electrical properties of squid axons. *Journal of Physiology.* 137:218–244.

Godt, R. E., and B. D. Lindley. 1982. Influence of temperature upon contractile activation and isometric force production in mechanically skinned muscle fibers of the frog. *Journal of General Physiology.* 80:279–297.

Gupta, R. K., J. L. Benovic, and Z. B. Rose. 1978. The determination of the free magnesium level in the human red blood cell by ^{31}P NMR. *Journal of Biological Chemistry.* 253:6172–6176.

Gupta, R. K., P. Gupta, and R. D. Moore. 1984. NMR studies of intracellular metal ions in intact cells and tissues. *Annual Review of Biophysics and Bioengineering.* 13:221–246.

Gupta, R. K., and W. D. Yushok. 1980. Non-invasive ^{31}P NMR probes of free Mg^{2+}, MgATP, and MgADP in intact Ehrlich ascites tumor cells. *Proceedings of the National Academy of Sciences.* 77:2487–2491.

Hadley, R. W., and J. R. Hume. 1987. An intrinsic potential-dependent inactivation mechanism associated with calcium channels in guinea-pig myocytes. *Journal of Physiology.* 389:205–222.

Hamill, O. P., A. Marty, E. Neher, B. Sakmann, and F. J. Sigworth. 1981. Improved patch-clamp techniques for high-resolution current recording from cells and cell-free membrane patches. *Pflügers Archiv.* 391:85–100.

Hartzell, H. C. 1989. Regulation of cardiac ion channels by catecholamines, acetylcholine, and second messenger systems. *Progress in Biophysics and Molecular Biology.* In press.

Hartzell, H. C., and R. Fischmeister. 1986. Opposite effects of cyclic GMP and cyclic AMP and Ca^{2+} current in single heart cells. *Nature* 323:273–275.

Hartzell, H. C., and R. Fischmeister. 1987. Effect of forskolin and acetylcholine on calcium current in single isolated cardiac myocytes. *Molecular Pharmacology.* 32:639–645.

Hartzell, H. C., and M. A. Simmons. 1987. Comparison of effects of acetylcholine on calcium and potassium currents in frog atrium and ventricle. *Journal of Physiology.* 389:411–422.

Henquin, J. C., T. Tamagawa, M. Nenquin, and M. Cogneau. 1983. Glucose modulates Mg^{2+} fluxes in pancreatic islet cells. *Nature.* 301:73–74.

Hess, P., P. Metzger, and R. Weingart. 1982. Free magnesium in sheep, ferret and frog striated muscle at rest measured with ion-selective micro-electrodes. *Journal of Physiology.* 333:173–188.

Hodgkin, A. L., and A. F. Huxley. 1952. A quantitative description of membrane current and its application to conduction and excitation in nerve. *Journal of Physiology.* 117:500–544.

Kass, R. S., and D. S. Krafte. 1987. Negative surface charge density near heart calcium channels. Relevance to block by dihydropyridines. *Journal of General Physiology.* 89:629–644.

Kass, R. S., and M. C. Sanguinetti. 1984. Inactivation of calcium channel current in calf cardiac Purkinje fiber. Evidence for voltage- and calcium-mediated inactivation. *Journal of General Physiology.* 84:705–726.

Kass, R. S., M. C. Sanguinetti, and D. S. Krafte. 1986. Inactivation and modulation of cardiac Ca channels. *In* Cardiac Muscle: The Regulation of Excitation and Contraction. R. D. Nathan, editor. Academic Press, Inc., New York, 29–53.

Lansman, J. B., P. Hess, and R. W. Tsien. 1986. Blockade of current through single calcium channels by Cd^{2+}, Mg^{2+}, and Ca^{2+}. Voltage and concentration dependence of calcium entry into the pore. *Journal of General Physiology.* 88:321–348.

Lee, K. S., E. Marban, and R. W. Tsien. 1985. Inactivation of calcium channels in mammalian heart cells: joint dependence on membrane potential and intracellular calcium. *Journal of Physiology.* 364:395–411.

Maguire, M. E. 1984. Hormone-sensitive magnesium transport and magnesium regulation of adenylate cyclase. *Trends in Pharmacological Sciences.* 5:73–77.

Maughan, D. 1983. Diffusible magnesium in frog skeletal muscle cells. *Biophysical Journal.* 43:75–80.

Mentrard, D., G. Vassort, and R. Fischmeister. 1984. Calcium-mediated inactivation of the calcium conductance in cesium-loaded frog heart cells. *Journal of General Physiology.* 83:105–131.

Mitra, R., and M. Morad. 1986. Two types of calcium channels in guinea pig ventricular myocytes. *Proceedings of the National Academy of Sciences.* 83:5340–5344.

Nilius, B., P. Hess, J. B. Lansman, and R. W. Tsien. 1985. A novel type of cardiac calcium channel in ventricular cells. *Nature.* 316:443–446.

Noma, A., H. Kotake, and H. Irisawa. 1980. Slow inward current and its role mediating the chronotropic effect of epinephrine in the rabbit sinoatrial node. *Pflügers Archiv.* 388:1–9.

Reuter, H. 1983. Calcium channel modulation by neurotransmitters, enymes and drugs. *Nature* 301:569–574.

Rosenberg, R. L., P. Hess, and R. W. Tsien. 1988. Cardiac calcium channels in planar lipid bilayers: L-type channels and calcium-permeable channels open at negative membrane potentials. *Journal of General Physiology.* 92:27–54.

Tillotson, D., 1979. Inactivation of Ca conductance dependent on entry of Ca ions in molluscan neurons. *Proceedings of the National Academy of Sciences.* 76:1497–1500.

Trautwein, W., and D. Pelzer. 1985. Gating of single calcium channels in the membrane of enzymatically isolated ventricular myocytes from adult mammalian hearts. *In* Cardiac Electrophysiology and Arrhythmias. D. P. Zipes and J. Jalife, editors. Grune & Stratton, Orlando, FL, 31–42.

Tsien, R. W. 1977. Cyclic AMP and contractile activity in heart. *Advances in Cyclic Nucleotide Research.* 8:363–340.

Tsien, R. W. 1983. Calcium channels in excitable cell membranes. *Annual Review of Physiology.* 45:341–358.

Tsien, R. W., B. P. Bean, P. Hess, J. B. Lansman, B. Nilius, and M. C. Nowycky. 1986. Mechanisms of calcium channel modulation by β-adrenergic agents and dihydropyridine calcium agonists. *Journal of Molecular and Cellular Cardiology.* 18:691–710.

Vassort, G., and O. Rougier. 1972. Membrane potential and slow inward current dependence of frog cardiac mechanical activity. *Pflügers Archiv.* 331:191–203.

Watanabe, Y., and L. S. Dreyfus. 1972. Electrophysiological effects of magnesium and its interactions with potassium. *Cardiovascular Research.* 6:79–88.

White, R. E., and H. C. Hartzell. 1988. Effects of intracellular free magnesium on calcium current in isolated cardiac myocytes. *Science.* 239:778–780.

White, R. E., and H. C. Hartzell. 1989. Magnesium ions in cardiac functions: regulator of ion channels and second messengers. *Biochemical Pharmacology.* 38:859–867.